2024 10th IEEE RAS/EMBS International Conference for
Biomedical Robotics and Biomechatronics (BioRob)
1-4 September 2024. Heidelberg, Germany

2024 10th IEEE RAS/EMBS International Conference for Biomedical Robotics and Biomechatronics (BioRob) | 979-8-3503-8652-3/24/$31.00 ©2024 IEEE | DOI: 10.1109/BIOROB60516.2024.10719791

A Modular, Time-Independent, Path-Based Controller for Assist-As-Needed Rehabilitative Exoskeletons

Giulia Bodo*,1,2, Raffaele Giannattasio*,3,2, Vishal Ramadoss[2], Federico Tessari[4] and Matteo Laffranchi[2]

***Abstract*— After a traumatic event (e.g., orthopedic or neurological injury), engaging in activities of daily living (ADLs) encourages the individual and aids in relearning functional motions for the impaired limb. The outcome of robot-assisted rehabilitation is inherently connected to the control strategy adopted in the training sessions. Here, the authors propose a time-independent path-tracking controller with impedance modulation that provides assistance and guidance along the path. Based on the assist-as-needed (AAN) paradigm, a task-space-based force field controller was designed to cooperatively support the individual during training. The authors will illustrate the flexibility of the proposed control strategy, showcasing its adaptability to various exoskeletons with minimal or minor adjustments. Leveraging the control versatility, the authors propose the application of this methods to two case studies: Float upper limb and TWIN lower limb exoskeletons.**

I. INTRODUCTION

In the last decade, various exoskeletons have been developed to provide assistance and guidance for the upper limb: AnyExo [1], Harmony [2], CleverArm [3], Float [4]; and the lower limb movement such as Hal [5], Indego [6], TWIN [7] and ReWalk[8]. Initially, these robotic devices exclusively guided patients along predetermined fixed paths without adjusting their movements based on the patient's activity. Position-controlled training of this kind is appropriate for individuals in the initial phases of rehabilitation [9]. However, the exoskeleton's rigid guidance is not suitable for patients with a certain level of volitional control. Current exoskeleton models are increasingly aligning with the concept of control based on assistance-as-needed (AAN) which is a form of patient-cooperative control strategy [9]. With the AAN control, the individual receives assistance to the minimal required extent, adhering to the principle of minimum intervention, thereby optimizing their inherent contribution. The initial endeavors focused on incorporating compliance in the devices. This was achieved by augmenting the exoskeletons with impedance control techniques [10]. However, methodologies employing traditional impedance control exhibit the drawback of imposing a predetermined timing of movements on the individual [11]. A possible approach to gain timing freedom, is by utilizing time-independent vector fields (TIVeF). A significant amount of research in TIVeF controls is implemented in the joint domain [6], [10]. A velocity field controller was augmented with a force field component to attain the AAN property in a lower limb exoskeleton [12]. Most research solutions for implementing AAN control within the joint domain revolve around the concept of a virtual tunnel, which defines an area/volume along the path where assistive control is applied [13], [14], [15]. Cartesian space control is prioritized over joint-space control due to its alignment with functional task requirements [16], [15], facilitating the distinction of robot assistance in both tangential and orthogonal directions concerning the end-effector reference motion. This functionality enables the robot to assist along the axial direction of motion and perform corrections along the radial direction. The authors propose an AAN control approach for rehabilitative exoskeletons that introduces the concept of a modular tunnel to compute task-based vector assistive force-fields and integrates them with time-independent path planning. This work focuses on designing these control algorithms as a general concept and implementing them on two different rehabilitative devices: the Float Upper-Limb exoskeleton [4] and the TWIN Lower-Limb exoskeleton [7].

II. CASE STUDIES

A. Float Upper-Limb exoskeleton

The Float exoskeleton prototype consists of 7 Degrees-of-Freedom (DoF), with inner and outer shoulder complex that allows scapular control. It is equipped with custom Series-Elastic-Actuators [17] to guarantee repeatable torque sensing capabilities and compliant control. In this preliminary exoskeleton testing, we narrowed down the analysis to four specific joints (J1,J4,J5,J6) out of the seven available. Three joints were immobilized, and torque control was applied to the remaining four. Thus, the experiments focused on a 4-DoF system, depicted in Figure 1, encompassing J1 for scapular retraction and protraction, as well as the spherical complex formed by J4, J5, and J6. These joints participate in shoulder flexion-extension, abduction-adduction, and internal-external rotation.

B. TWIN Lower-Limb exoskeleton

TWIN is an active lower-limb exoskeleton consisting of a main pelvis component with actuated modules for thighs and shanks corresponding to right and left leg. The sizes are customizable according to the user. Each leg consists of two

* Co-First authors, equal contribution
[1]PhD student in Mechanical Engineering at Politecnico di Torino, Torino, Corso Duca degli Abruzzi 24, 10129, Italy.
[2]Rehab Technologies Laboratory at Istituto Italiano di Tecnologia, Genova, Via Morego 30, 16163, Italy.
[3]PhD student in Biomedical Engineering at Politecnico di Milano, Milano, Via Giuseppe Ponzio, 34, 20133, Italy
[4]Postdoctoral Associate, Mechanical-Mechatronic Engineer The Eric P. and Evelyn E. Newman Laboratory for Biomechanics and Human Rehabilitation Department of Mechanical Engineering Massachusetts Institute of Technology.

active DoFs (hip and knee) and a passive joint for the ankle-foot-complex (AFO). Strain gauges are employed to measure the forces and joint torques in the lower-limb exoskeleton.

III. CONTROL DESIGN

The design combines: Cartesian-space assistance, joint-level impedance, gravity, and friction compensation algorithms to implement an Assist as Needed control strategy for upper and lower limb exoskeleton applications. The proposed control system aims to enable patients to understand the correct path to follow thanks to the feedback provided by the assistance at the end-effector. This assistance is provided within a tunnel of variable diameter centered on the reference path, allowing customizable user assistance based on the current position. The control algorithm includes gravity and friction compensation for seamless exoskeleton movement, ensuring a transparent user experience. Additionally, joint impedance control is used to optimize torque management.

The proposed method involves the following steps: (I) defining a reference path for the end-effector and approximating it with a parameterized curve; (II) identifying the tunnel where assistance is provided; (III) computing the actual position of the end-effector by leveraging direct kinematics; (IV) determining the minimum distance point on the reference path concerning the current end-effector position; (V) computing the assistive contribution at the end-effector; (VI) implementing joint-level impedance and computing torque contributions for gravity and friction compensations.

A. Reference paths

Reference paths are defined for both upper and lower limb exoskeletons. For the upper limb, a flexion movement is presented as a case study. To define the proposed reference trajectory, scapular and rotational movements were kept fixed to obtain pure shoulder flexion on the defined plane (30 degrees open with respect to the sagittal plane). For the lower limb exoskeleton the provided reference is the walk gait path implemented in TWIN exoskeleton control [18]. Paths were defined taking into account variable link sizes based on user anthropometry: the 1st (S), 50th (M), and 99th (L) male percentiles are represented in Figure 1.

B. Path parametrization and tunnel

A conic curve approximation was used to parametrize the reference path. For upper limb flexion path, the computed fitting is represented by a degenerate ellipse i.e., a circumference.

For the lower limb walking gait, the path is defined using the ellipse that best approximates the desired path in a least squares sense, as proposed in [19]. This elliptical approximation is chosen due to the highly elliptical shape of TWIN gait trajectories proposed in [18]. The resulting maximum approximation error is $2mm$, closely resembling the original path. Considering the ellipse parametric equations in polar form rotated by an angle Φ:

$$\begin{aligned} x_r &= x_0 + a \cdot \cos(\varphi) \\ y_r &= y_0 + b \cdot \sin(\varphi) \end{aligned} \tag{1}$$

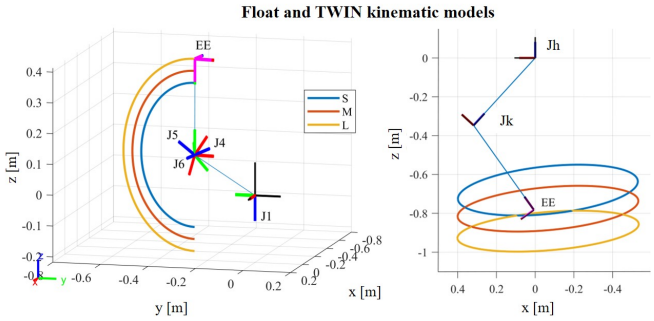

Fig. 1. Float (on the left): exploring shoulder flexion paths in the sagittal plane within Cartesian space, varying link sizes (S, M, L). J1 aligns with the fixed base, focusing on scapular motion. J4, J5, and J6 represent the glenohumeral joints, facilitating diverse shoulder movements. The End-Effector (EE) is positioned at elbow level.TWIN (on the right): highlighting hip (Jh) and knee (Jk) joints, with the EE located at the malleolus. The illustrated walking path is approximated by an ellipse and it showcases the variations across different anthropometries.

$$R = \begin{bmatrix} \cos(\Phi) & \sin(\Phi) \\ -\sin(\Phi) & \cos(\Phi) \end{bmatrix} \tag{2}$$

where (x_0, y_0) and (x_r, y_r) are respectively, the coordinates of the center of the ellipse and the points of the ellipse itself, a is the semi-major axis, and b is the semi-minor axis. $\varphi \in [0, 2\pi]$ is the angle used to parametrize the ellipse. After the parametrization the deduced set of equations (Eq: 1) was multiplied by the rotational matrix R (Eq: 2), to obtain the ellipse correct orientation. The approximated curves can be represented with the parameters collected in Table I.

	$a[m]$	$b[m]$	$\Phi[rad]$	$x_0[m]$	$y_0[m]$	$z_0[m]$
Float	0.3096	0.3096	0.0	-	-0.3059	0.0946
TWIN	0.4693	0.0986	0.0797	0.0044	-	-0.8942

TABLE I
ELLIPSE PARAMETERS FOR FLOAT AND TWIN EXOSKELETONS PATHS.

1) Float case: The Float Exoskeleton is designed to support shoulder rehabilitation. The proposed control system focuses on developing an assistive field to guide users through simple tasks, such as shoulder flexion, which is essential for many ADLs. Float's selected joints (J1,J4,J5,J6) can navigate the Cartesian space across three coordinates. A control tunnel with variable diameter was designed to reproduce shoulder flexion. Inside, movement assistance is provided, by means of a push in the direction of the tunnel main axis. Our design decision was to offer assistance within a wider tunnel at the trajectory extremes, while narrowing it around 90 degrees. This ensures that the feedback provided to the user (in the form of a push) encourages them to maintain movement on the predefined sagittal plane, particularly at 90 degrees where the load force is at its maximum. As shown in Figure 2a the tunnel diameter d_t varies within a specified range, from $0.10m$ to $0.30m$, following the relationship: $d_t = (0.1 + 0.2 \cdot |sin(\varphi)|)[m]$.

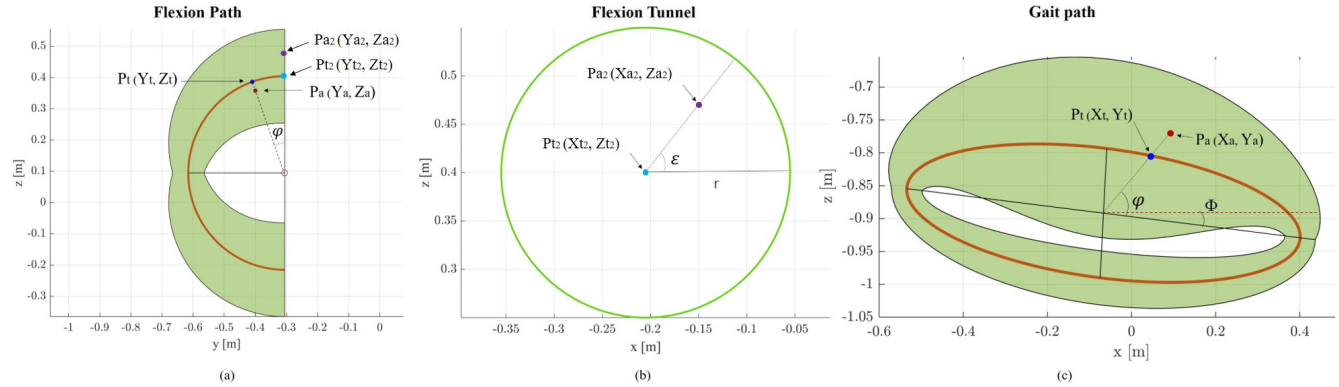

Fig. 2. Reference end-effector trajectories (obtained with ellipse parametrization) for Float and Twin, specifically: (a) Float tunnel section (green) on the YZ plane of flexion path (red). (b) Tunnel section at max diameter for assistance (case of 180 deg of flexion), with the reference trajectory point (*t2*) in light blue. The violet marker denotes the current end-effector position (*a2*). Assistance is provided only inside the tunnel based on the Euclidean norm between the coordinates. (c) TWIN reference path (red), and its tunnel in Cartesian space (green). The tunnel changes its shape according to the gait phase (support/swing) and the angle φ. Assistance is provided only inside the tunnel based on the Euclidean norm between the coordinates.

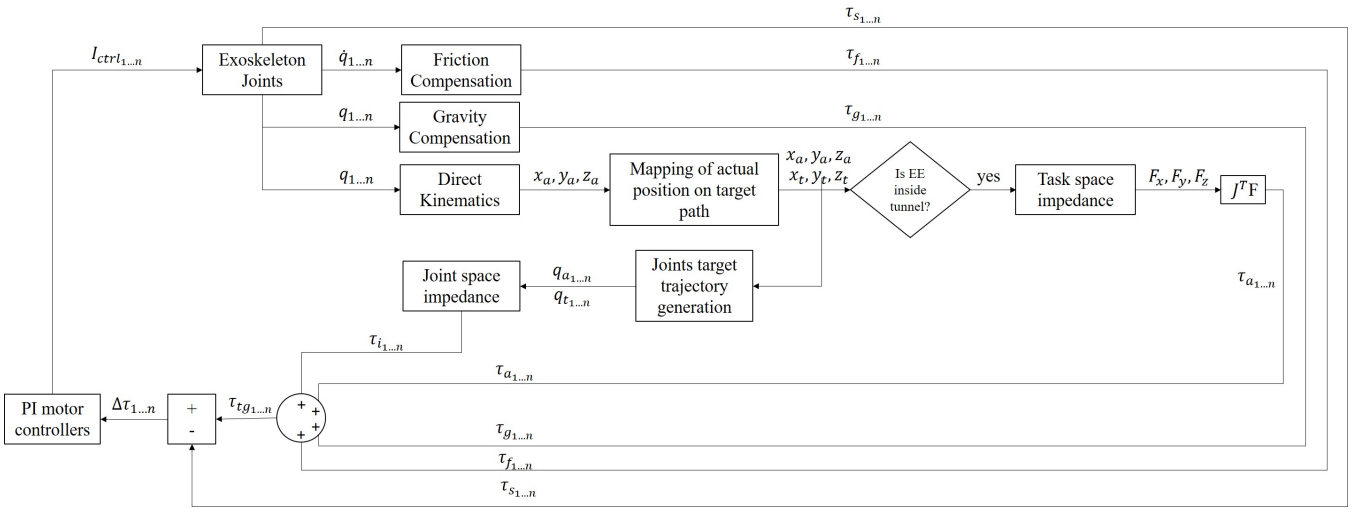

Fig. 3. Control algorithm for implementing time-independent assist-as-needed mode in the task space. Parameters such as joint position, velocity, and estimated torque contribute to gravity, friction, and assistance compensations. Forward kinematics calculates the end-effector pose, mapped onto the reference trajectory to determine assistance (force in task space, translated to joint torque via transposed Jacobian). Joint level impedance can be implemented to provide additional guidance. Contributions sum up following superposition principle, yielding the reference control torque.

2) TWIN case: The TWIN gait is executed in a 2D space. The proposed tunnel has been designed to allow greater movement deviation from the reference during the swing phase, while restricting freedom during the stance phase to ensure contact between the exoskeleton and the ground. The variable diameters of the tunnel follow the relationships:

- $d_{t_{st}} = (7 + 1 \cdot |sin(\varphi)|) \cdot 10^{-2}[m]$ for stance phase
- $d_{t_{sw}} = (7 + 20 \cdot |sin(\varphi)|) \cdot 10^{-2}[m]$, for swing phase

ranging from a minimum of $7 \cdot 10^{-2}m$ to $8 \cdot 10^{-2}m$ (in stance phase) and to $27 \cdot 10^{-2}m$ (in swing phase), the design is shown in Figure 2c.

C. Mapping of actual position on the reference path

Once the actual end-effector pose is known, we propose to map its coordinates onto the reference path. The nearest point to the actual position on the reference path is assumed to correspond to the intersection between the reference path (ellipse) and the line passing through both the ellipse center and the actual position, as illustrated in Figure 2a and 2c . The same level of assistance will be provided for all actual points lying on this line, following the direction of the reference path. Once the corresponding point on reference path (X_t, Z_t) is defined, it is required to determine whether assistance needs to be provided or not, a Euclidean norm is computed to verify that the distance of the end-effector (X_a, Z_a) from the center of the tunnel, (X_t, Z_t) is smaller than the tunnel radius (r), as shown in Figure 2b.

D. Assist as Needed: task space impedance

Task space impedance allows the design of interaction forces applied at the end-effector level by exploiting a spring-damper dynamic model. For the Float exoskeleton, the end-effector was considered at the elbow level, while for the TWIN, it was positioned at the malleolus. Stiffness and

damping matrices have been tuned to realize at the maximum distance (i.e., the tunnel radius) a force of $\pm 3N$ and $\pm 4N$ to be applied at the exoskeleton end-effector for the Float and TWIN systems, respectively. For the showcase implementation, the problem has been simplified, considering only diagonal elements for stiffness and damping matrices. The task space forces can be computed as:

$$\begin{bmatrix} F_x \\ F_y \\ F_z \end{bmatrix} = K \cdot \begin{bmatrix} \Delta x \\ \Delta y \\ \Delta z \end{bmatrix} + B \cdot \begin{bmatrix} \dot{x} \\ \dot{y} \\ \dot{z} \end{bmatrix} \tag{3}$$

where,

$$K = \begin{bmatrix} k_{xx} & 0 & 0 \\ 0 & k_{yy} & 0 \\ 0 & 0 & k_{zz} \end{bmatrix} and\ B = \begin{bmatrix} \beta_{xx} & 0 & 0 \\ 0 & \beta_{yy} & 0 \\ 0 & 0 & \beta_{zz} \end{bmatrix} \tag{4}$$

are stiffness and damping matrices, $\Delta x, \Delta y, \Delta z$ are the difference between coordinates of the next target on the reference path and the actual ones, and $\dot{x}, \dot{y}, \dot{z}$ are the end-effector actual speed components. The forces computed in task space can be translated into joint torques by leveraging the Jacobian transpose. In a system with *n* joints and *m* degrees of freedom, this relationship can be expressed as follows:

$$\tau_{a_{(n,1)}} = J^T_{(n,m)} \cdot F_{(m,1)} \tag{5}$$

E. Joint space Impedance

Joint space impedance can be computed to introduce an additional corrective effect to the end-effector position with respect to a desired reference. To avoid going through the inverse kinematics problem and related Jacobian inverse, the joint reference position can be arbitrarily set within a reasonable range around the current joint position. Subsequently, a low-stiffness impedance can be implemented, encouraging subjects to maintain the exoskeleton joints close to these values. Thus, imposing stiffness (k_j) and damping (β_j) coefficients, joint level impedance control can be implemented as:

$$\tau_{i_{(1\dots n)}} = k_j \cdot \Delta q_{(1\dots n)} + \beta_j \cdot \dot{q}_{(1\dots n)} \tag{6}$$

F. Gravity and Friction compensation

Gravity compensation is computed using the dynamic model of the two exoskeletons. Once the joint configuration, mass, and inertial properties of each link are obtained (derived from geometric models), the torques induced by gravity can be computed. To estimate and compensate for frictions at the joint levels, the observer algorithm proposed by Le Tien et al. in [20] has been implemented.

G. Application of superposition principle in computing reference torques

The low-level control strategy employs a closed-loop Proportional-Integral (PI) torque controller. Torque feedback is obtained from the torque sensors in the SEA joints for the Float case and from strain gauge torque sensors in the TWIN exoskeleton. The reference torque control signal is composed of: task space based assistance torque τ_a, joint level impedance τ_i, gravity torque τ_g and friction compensation τ_f. The resulting reference torque required at each joint can be computed as:

$$\tau_{tg_{(1\dots n)}} = \tau_{a_{(1\dots n)}} + \tau_{i_{(1\dots n)}} + \tau_{g_{(1\dots n)}} + \tau_{f_{(1\dots n)}} \tag{7}$$

IV. RESULTS

The proposed control system was implemented in C++ for embedded solutions and tested on the Float and Twin exoskeletons. For both exoskeletons, the reference path and the machine were adjusted for a L size with reference to Figure 1.

A. Assist-as-Needed Test: Float Case Study

The exoskeleton was operated with the activated Assist-As-Need strategy. The results are presented for two experiments: Test1, where flexion was performed within the tunnel, and Test2, where the end effector was moved inside and outside the tunnel to assess AAN contributions. In Figure 4, the blue line represents the reference path, and the green area denotes the implemented assistive tunnel. The yellow trajectory illustrates the end-effector's path during the test, with (for Test1) start and end points of flexion movements from -20 to 130 degrees. AAN support activates only if the end effector stays within the predefined tunnel. Figure 5 displays the computed end-effector force components and corresponding joint torques.

B. Assist-as-Needed Test: TWIN Case Study

For a preliminary validation of the implemented control strategy, the lower limb exoskeleton was secured on a stander to prevent ground contact of the limbs. An external operator manipulated the end-effector of one leg to simulate a walking gait. Figure 6 illustrates the reference elliptical path depicted in red, with the green region indicating the implemented assistive tunnel. In yellow the path followed by the end-effector during the test. AAN is provided only within the tunnel (assistive force is shown in blue).

V. DISCUSSION

The proposed control strategy has been implemented in two exoskeletons: Float and TWIN. For the Float upper-limb exoskeleton, the results demonstrate how the proposed algorithm correctly identifies the position of the end effector relative to the virtual tunnel (Figure 4) and calculates the corresponding AAN contribution (Figure 5). For these preliminary results, the same combinations of k and β were adopted for the three force components ($k_{xx} = k_{yy} = k_{zz} = 50N/m$, $\beta_{xx} = \beta_{yy} = \beta_{zz} = 3N \cdot s/m$). The assistance correctly provides support along the direction of movement. During Test 1 (Figure 4 Test 1), the main force component is Fz, indicating that the movement direction is indeed flexion. The resulting predominant torque is at joint J6, which, in the proposed kinematics, has the greatest influence on flexion. The contribution to other joints is justified because the movement does not perfectly follow the reference path plane, resulting in minor components along

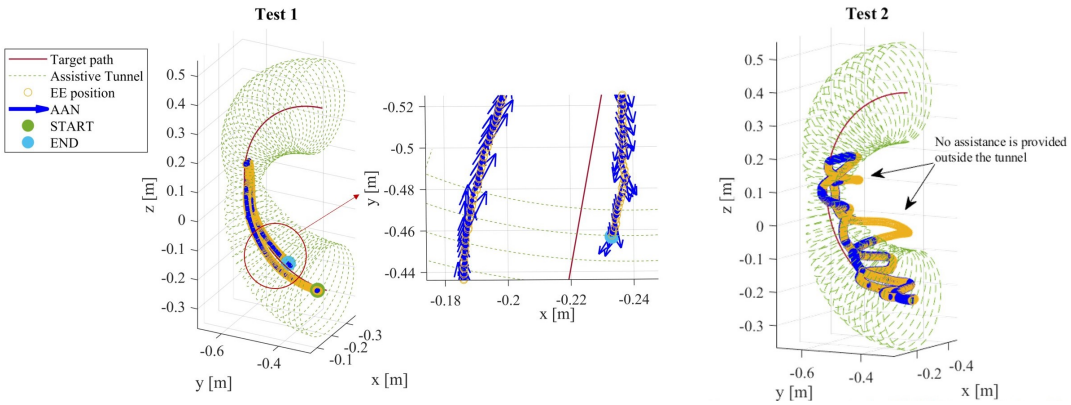

Fig. 4. Results from the experimental test on the upper limb exoskeleton are presented. Blue and yellow data are collected In Test1, a flexion was executed while staying inside the tunnel, depicting the reference (blue) and actual (yellow) paths. Assist-as-needed (AAN) forces are applied at the end effector, aiding in the movement performance in both directions (flexion-extension). Test2 demonstrates that AAN is exclusively applied inside the tunnel.

x and y, affecting J1, J4, and J5. During Test 2 (Figure 4 Test 2), the end effector was moved inside and outside the tunnel, especially using the scapular joint. In this case, the main force component is Fx, and the highest torque is on J1. From this behavior, it is evident how the force components along x and y could also play a corrective role, counteracting the exit from the tunnel and preventing the user from deviating too far from the reference path. In subsequent work, the Fx and Fy components could be tuned to oppose movements aiming outside the tunnel. The feasibility of the proposed Assist-As-Needed (AAN) control algorithm extends to the TWIN lower limb exoskeleton. In this scenario, the algorithm successfully identifies the nearest point on the reference path for computing assistance

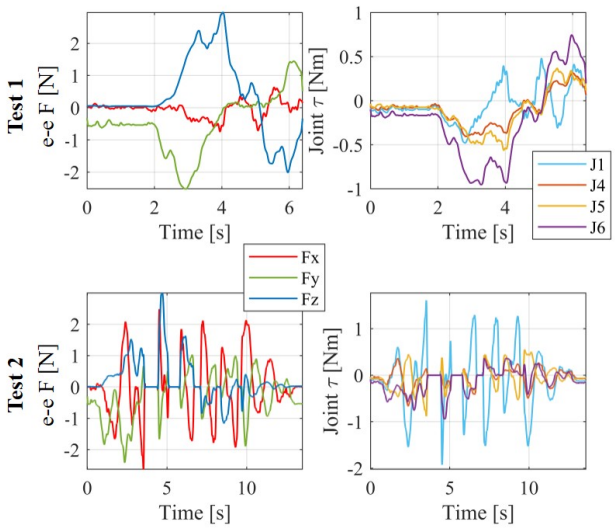

Fig. 5. The assistance was designed to provide a torque contribution of approximately ±2 Nm at the joint level. The figure shows at the left the x, y, and z components of the force that need to be applied at the end-effector to deliver the intended assistance. On the right, the computed joint torques necessary to achieve this force are displayed.

within the designated tunnel (Figure 6). Figure 6 illustrates the assistive force applied at the end-effector, depicted as a vector aligned with the reference direction of motion. The resulting joint torques facilitate hip extension during the support phase and hip and knee flexion during swing, aligning with the biomechanics of human gait. In terms of force magnitude, the same combinations of k and β ($k_{xx} = k_{zz} = 50N/m$, $\beta_{xx} = \beta_{zz} = 3N \cdot s/m$), were adopted for the two force components. In future work, the author plans to test the overall proposed algorithm (Figure 3) integrating the joint space impedance strategy thereby offering additional user guidance. A potential improvement involves introducing the capability to personalize human-robot interaction (HRI) by implementing variable, path-phase-dependent assistance through the modulation of impedance in Cartesian space. For instance, the control could provide more assistance during flexion i.e., when the arm is forwardly extended, to help overcoming the gravitational load. Further developments include integrating the assistive effect within the tunnel with an external corrective force. This external correction aims to guide the end-effector back into the predefined tunnel in case of deviation from the desired path.

VI. CONCLUSION

The presented work introduces a compliant control strategy suitable for implementing assist-as-needed modes in rehabilitative robotics. The incorporation of assistive forces not only caters to clinical needs but also engages users, encouraging them to follow the correct path during exercises. The proposed algorithm, combines both task-space and joint-level impedance controls, offering adaptability to physiological requirements through customizable assistive tunnels and reference trajectories. Moreover the concept of variable diameter tunnels, offers a versatile and adaptive framework for exoskeleton control, enabling the modulation of user freedom based on the reference position in Cartesian space. The proposed application examples for both upper and lower limb exoskeletons underscore its broad applicability. The use of impedance control provides a valuable method to overcome the risks related to inverse kinematics,

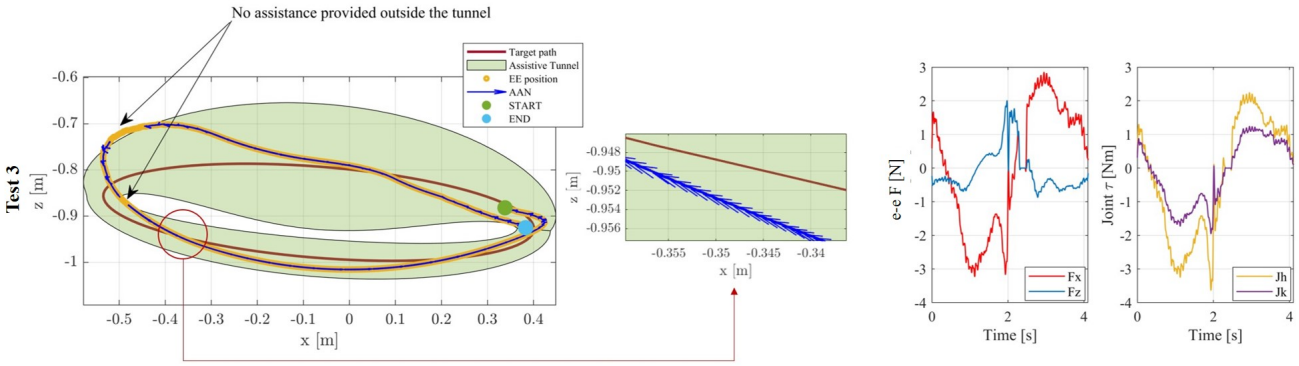

Fig. 6. Experimental results for the lower limb exoskeleton: the followed path is shown in yellow, extending both inside and outside the assistive tunnel (green) but receiving assistance (blue) only when inside it. The end-effector forces follow the direction of the reference path (red) from the start to the endpoints. The virtual applied forces Fx and Fz are shown, along with their mapping into the joint domain. To implement low to medium assistance, it was empirically estimated that the joint torque should be in the order of ±4 Nm at the joint level.

and in general Jacobian inversion. This not only enhances computational efficiency but also reduces the computational and physical risks related to singular configurations, thus improving users' and machine safety. Furthermore, the integration of controllable freedom through the tunnels allows for a more personalized experience, steering towards more patient-centric and adaptable robotic interventions.

ACKNOWLEDGMENT

This work was funded by the Istituto Nazionale per l'Assicurazione contro gli Infortuni sul Lavoro (INAIL) under grant agreements "PR19-RR-P2 - RoboGYM", and " PR19-RR-P1 - TwinMED".

REFERENCES

[1] Y. Zimmermann, M. Sommerhalder, P. Wolf, R. Riener, and M. Hutter, "Anyexo 2.0: A fully actuated upper-limb exoskeleton for manipulation and joint-oriented training in all stages of rehabilitation," *IEEE Transactions on Robotics*, 2023.

[2] B. Kim and A. D. Deshpande, "An upper-body rehabilitation exoskeleton harmony with an anatomical shoulder mechanism: Design, modeling, control, and performance evaluation," *The International Journal of Robotics Research*, vol. 36, no. 4, pp. 414–435, 2017.

[3] A. Zeiaee, R. S. Zarrin, A. Eib, R. Langari, and R. Tafreshi, "Cleverarm: A lightweight and compact exoskeleton for upper-limb rehabilitation," *IEEE Robotics and Automation Letters*, vol. 7, no. 2, pp. 1880–1887, 2021.

[4] S. Buccelli, F. Tessari, F. Fausto, L. D. Guglielmo, and G. C. et Al., "A gravity-compensated upper-limb exoskeleton for functional rehabilitation of the shoulder complex," *Applied Sciences*, vol. 12, no. 7, 2022.

[5] H. Kawamoto, S. Taal, H. Niniss, T. Hayashi, K. Kamibayashi, K. Eguchi, and Y. Sankai, "Voluntary motion support control of robot suit hal triggered by bioelectrical signal for hemiplegia," *2010 Annual international conference of the IEEE engineering in medicine and biology*, pp. 462–466, 2010.

[6] A. Martinez, B. Lawson, and M. Goldfarb, "A controller for guiding leg movement during overground walking with a lower limb exoskeleton," *IEEE Transactions on Robotics*, vol. 34, no. 1, pp. 183–193, 2017.

[7] M. Laffranchi, S. D'Angella, C. Vassallo, C. Piezzo, M. Canepa, S. De Giuseppe, M. Di Salvo, A. Succi, S. Cappa, G. Cerruti, *et al.*, "User-centered design and development of the modular twin lower limb exoskeleton," *Frontiers in neurorobotics*, vol. 15, p. 709731, 2021.

[8] A. Esquenazi, M. Talaty, A. Packel, and M. Saulino, "The rewalk powered exoskeleton to restore ambulatory function to individuals with thoracic-level motor-complete spinal cord injury," *American journal of physical medicine and rehabilitation*, vol. 91, no. 11, pp. 911–921, 2012.

[9] T. Proietti, V. Crocher, A. Roby-Brami, and N. Jarrasse, "Upper-limb robotic exoskeletons for neurorehabilitation: A review on control strategies.," *IEEE Rev Biomed Eng.*, vol. 9, pp. 4–14, Apr. 2016.

[10] A. Duschau-Wicke, J. Von Zitzewitz, A. Caprez, L. Lunenburger, and R. Riener, "Path control: a method for patient-cooperative robot-aided gait rehabilitation," *IEEE transactions on neural systems and rehabilitation engineering*, vol. 18, no. 1, pp. 38–48, 2009.

[11] R. Riener, L. Lunenburger, S. Jezernik, M. Anderschitz, G. Colombo, and V. Dietz, "Patient-cooperative strategies for robot-aided treadmill training: first experimental results," *IEEE transactions on neural systems and rehabilitation engineering*, vol. 13, no. 3, pp. 380–394, 2005.

[12] H. J. Asl and T. Narikiyo, "An assistive control strategy for rehabilitation robots using velocity field and force field," in *2019 IEEE 16th International Conference on Rehabilitation Robotics (ICORR)*, pp. 790–795, IEEE, 2019.

[13] H. I. Krebs, J. J. Palazzolo, L. Dipietro, M. Ferraro, J. Krol, K. Rannekleiv, B. T. Volpe, and N. Hogan, "Rehabilitation robotics: Performance-based progressive robot-assisted therapy," *Autonomous robots*, vol. 15, pp. 7–20, 2003.

[14] T. Proietti, V. Crocher, A. Roby-Brami, and N. Jarrasse, "Upper-limb robotic exoskeletons for neurorehabilitation: a review on control strategies," *IEEE reviews in biomedical engineering*, vol. 9, pp. 4–14, 2016.

[15] S. Dalla Gasperina, L. Roveda, A. Pedrocchi, F. Braghin, and M. Gandolla, "Review on patient-cooperative control strategies for upper-limb rehabilitation exoskeletons," *Frontiers in Robotics and AI*, vol. 8, p. 745018, 2021.

[16] T. Nef, M. Mihelj, G. Kiefer, C. Perndl, R. Muller, and R. Riener, "Armin-exoskeleton for arm therapy in stroke patients," in *2007 IEEE 10th international conference on rehabilitation robotics*, pp. 68–74, IEEE, 2007.

[17] G. Bodo, F. Tessari, S. Buccelli, L. De Guglielmo, G. Capitta, M. Laffranchi, and L. De Michieli, "Customized series elastic actuator for a safe and compliant human-robot interaction: Design and characterization," in *2023 International Conference on Rehabilitation Robotics (ICORR)*, pp. 1–6, IEEE, 2023.

[18] M. Zuccatti, G. Zinni, S. Maludrottu, V. Pericu, M. Laffranchi, A. Del Prete, L. De Michieli, and C. Vassallo, "Modeling the human gait phases by using bèzier curves to generate walking trajectories for lower-limb exoskeletons," pp. 1–6, Sept. 2023.

[19] G. Ohad, "fitellipse," *MATLAB Central File Exchange*, 2024.

[20] L. Le Tien, A. Albu-Schaffer, A. De Luca, and G. Hirzinger, "Friction observer and compensation for control of robots with joint torque measurement," in *2008 IEEE/RSJ International Conference on Intelligent Robots and Systems*, pp. 3789–3795, 2008.